Support information

Sugar Blower Protocol Enabling Superior Electromagnetic Wave Absorption of Porous Micro Pipeline Carbon Materials

Chunyan Ding,[*, a,d,e,†] *Songsong Wu,*[*, a,d,†] *Yu Zhang,*[a] *Yun Wu,*[a] *Xin Geng,*[a] *Xiaoxiao Huang,,*[c] *Guangwu Wen,*[*, a,b,d,e], *and Anying Wang*[e]

[a] School of Materials Science and Engineering, Shandong University of Technology, Zibo 255000, P.R. China

[b]School of Materials Science and Engineering, Harbin Institute of Technology at Weihai, Weihai 264209, P.R. China

[c]School of Materials Science and Engineering, Harbin Institute of Technology, Harbin 150001, P. R. China

[d]Shandong Industrial Ceramics Research & Design Institute Co., Ltd., Zibo 255000, P. R. China

[e]Shandong Institute of Advanced Ceramics Co. LTD, China

* Contact Number: (+86)15166110288 (G.W. Wen), (+86) 15098118986 (C.Y. Ding), (+86) 15552670275 (S.S. Wu)

*To whom correspondence should be addressed: wenguangwu2018@126.com (G. W. Wen); dcy@sdut.edu.cn (C. Y. Ding); wuss@sdut.edu.cn(S. S. Wu)

[†]These authors contribute equally to this work as the first authors.

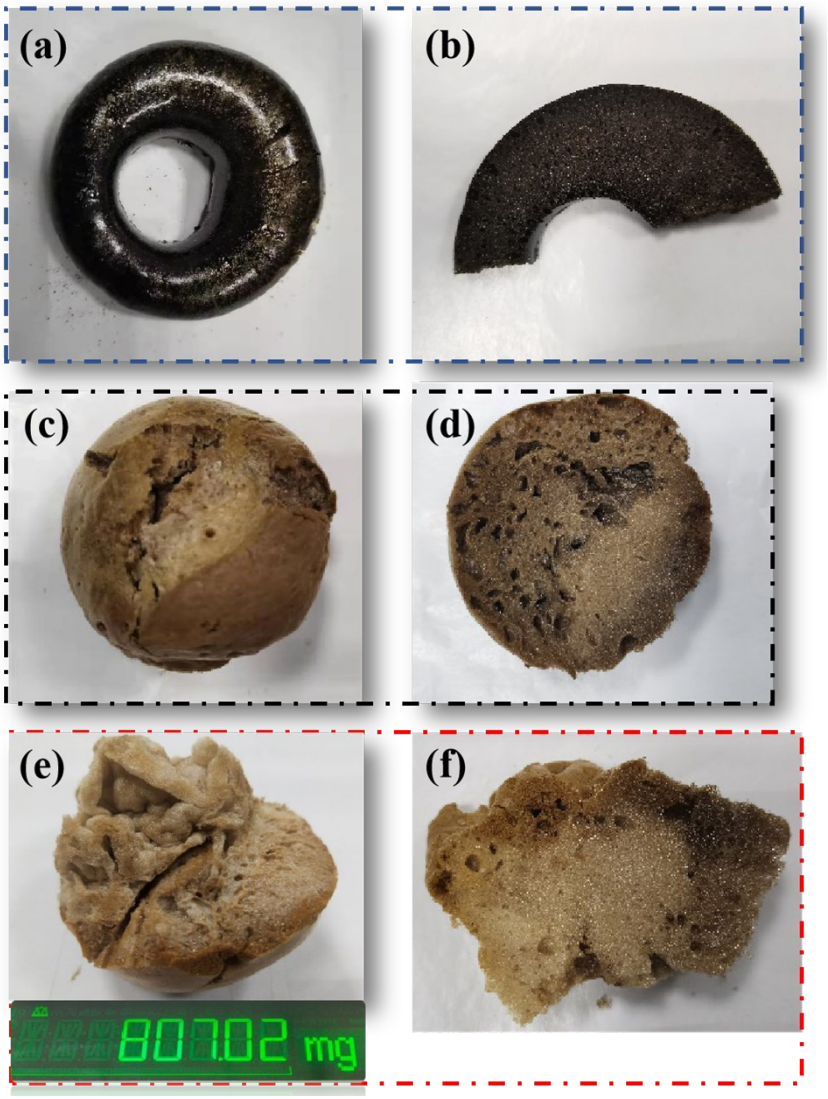

Fig. S1. The photographs of precursor of PMPC-1.5 (a), PMPC-2.0 (c), PMPC-2.5 (e), side profile of precursor of PMPC-1.5 (b), PMPC-2.0 (d), PMPC-2.5 (f).

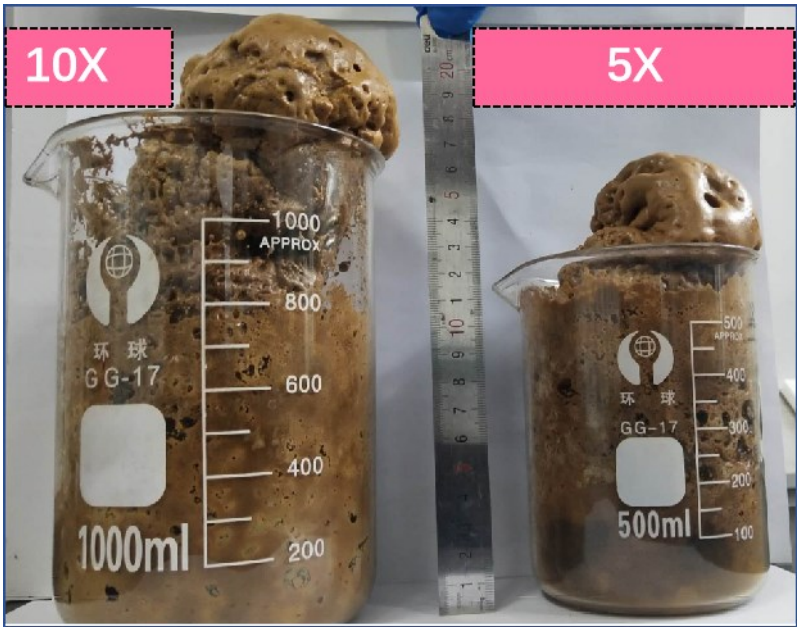

Fig. S2. The photographs of scale-up precursor production of five times and ten times.

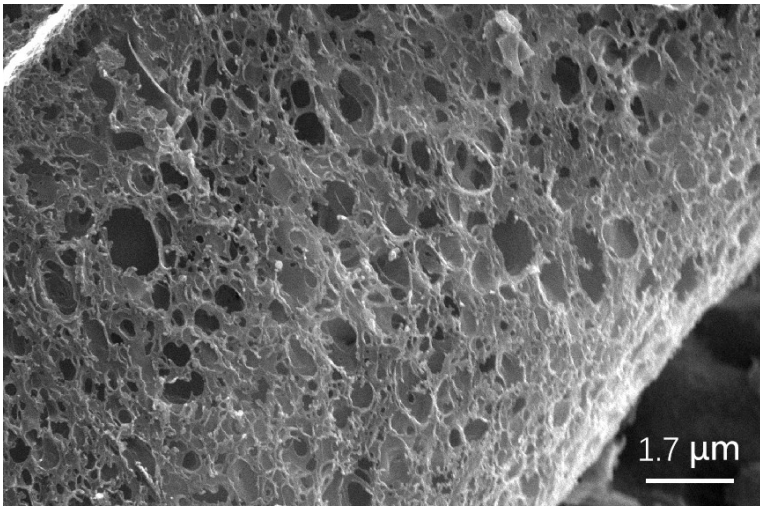

Fig. S3. SEM image of the surface topography for PMPC-2.5.

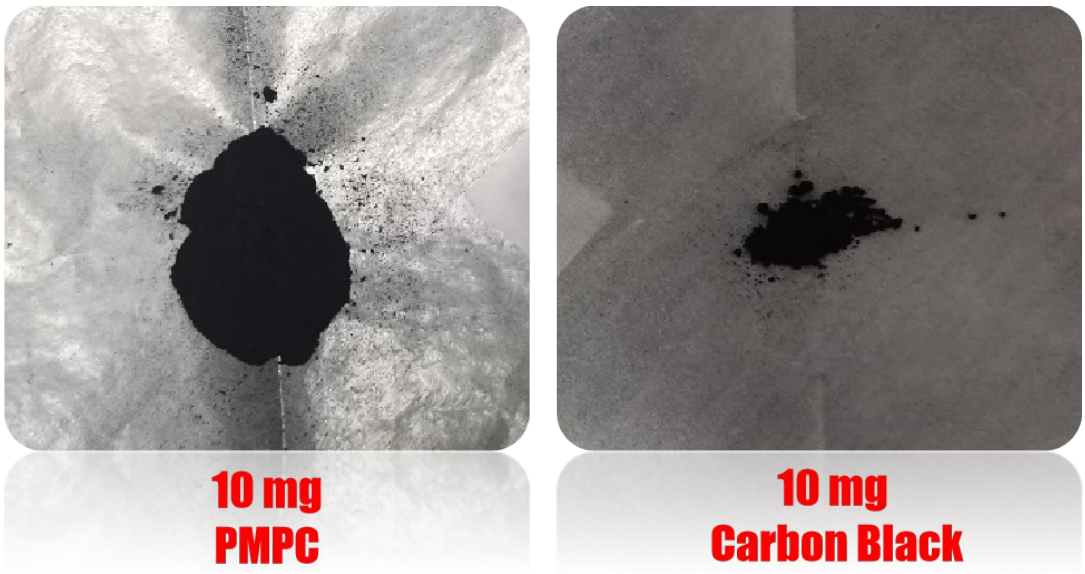

Fig. S4. The photographs of 10 mg PMPC-2.5 (a) and 0.01g carbon black (CARBOT) (b).

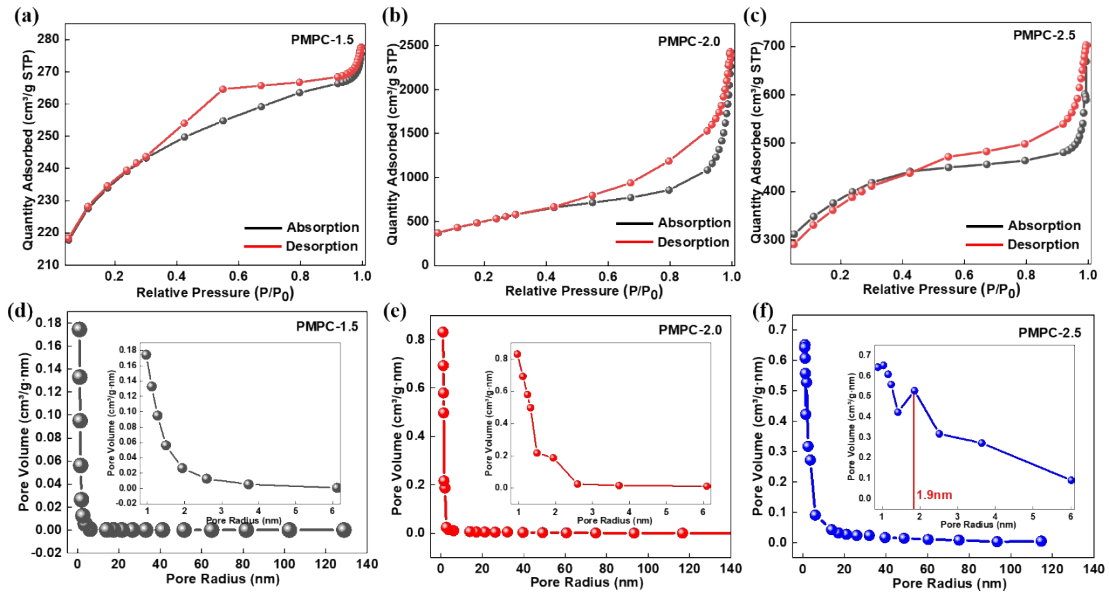

Fig. S5. N_2 adsorption-desorption isotherms of (a) PMPC-1.5, (b) PMPC-2.0, (c) PMPC-2.5; the pore distribution (c) PMPC-1.5, (d) PMPC-2.0, (e) PMPC-2.5.

The specific surface area and the pore distribution of the PMPCs was examined by N_2 adsorption-desorption curves shown in Fig S5. The specific surface areas for PMPC-1.5, PMPC-2.0, and PMPC-2.5 are 729 m^2/g, 1280 m^2/g, and 1806 m^2/g, respectively. For the pore size distribution, all the PMPCs have micropores (< 2 nm) and mesopores (2-50 nm). However, the micropore volume can be calculated to be 0.43 m^3/g, 1.09 m^3/g, 3.64 m^3/g, respectively. This can be attributed to the different degree of activation under different zinc nitrate supplemental levels.

In a typical synthesis protocol, the complex of glucose and zinc ions is *in-situ* blown into the precursor with macropore pipelines, and zinc oxide produced in the later carbonization process can *in-situ* etch the pipeline surfaces producing large amounts of surface pores. Meanwhile, gases (CO_2, NO_2, NO) deriving from the cracking of oxygen-containing groups, can further activate the sample to produce a large number of micropores and mesopores. Therefore, the amount of zinc nitrate will greatly affect the pore configuration of the final products.

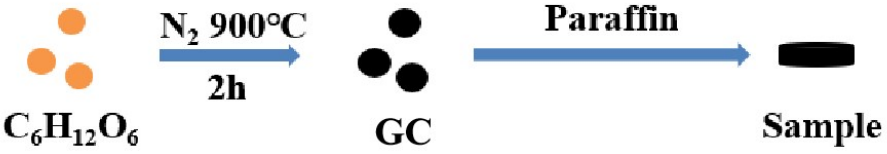

Fig. S6. Preparation process of glucose derived carbon (GC).

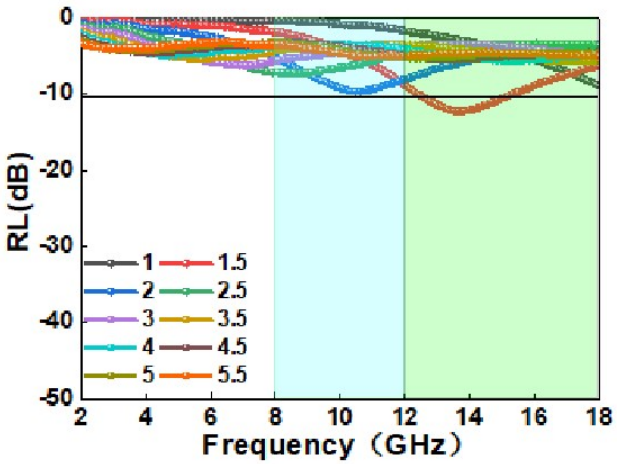

Fig. S7. EWA performance of GC.

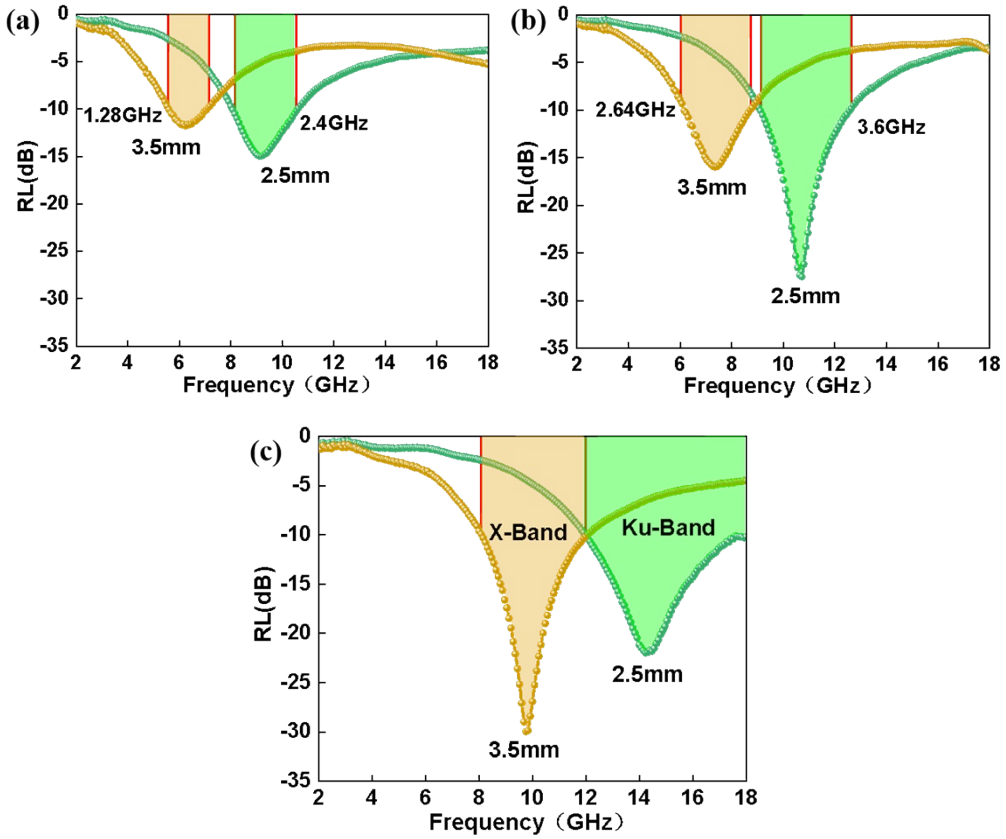

Fig. S8. RL *versus* frequency at the thickness of 2.5 mm and 3.5 mm: PMPC-1.5 (a), PMPC-2.0 (b) and PMPC-2.5 (c).

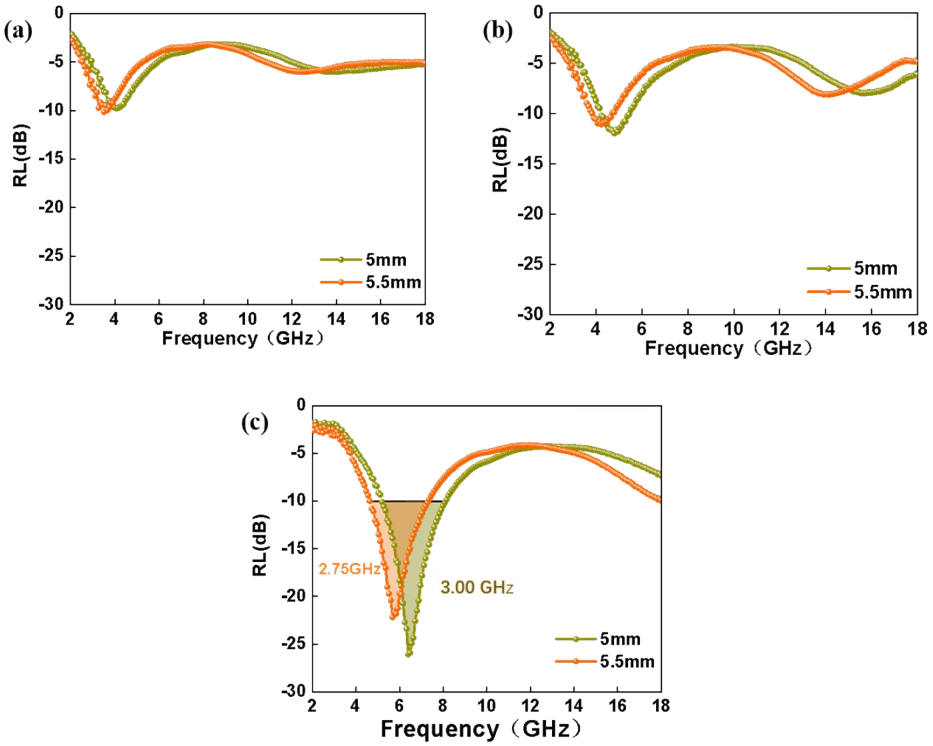

Fig. S9. RL values *versus* frequency at the thickness of 5.0 mm and 5.5 mm: PMPC-1.5 (a), PMPC-2.0 (b), PMPC-2.5 (c).

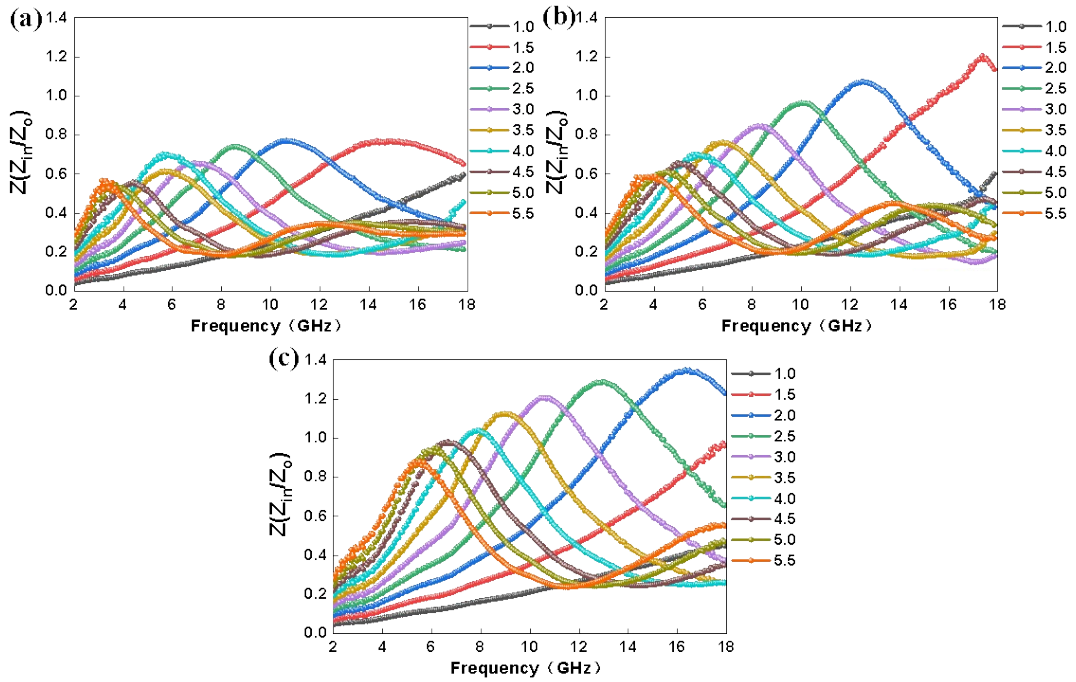

Fig. S10. Z (Z_{in}/Z_o) of PMPC-1.5 (a), PMPC-2.0 (b), PMPC-2.5 (c).

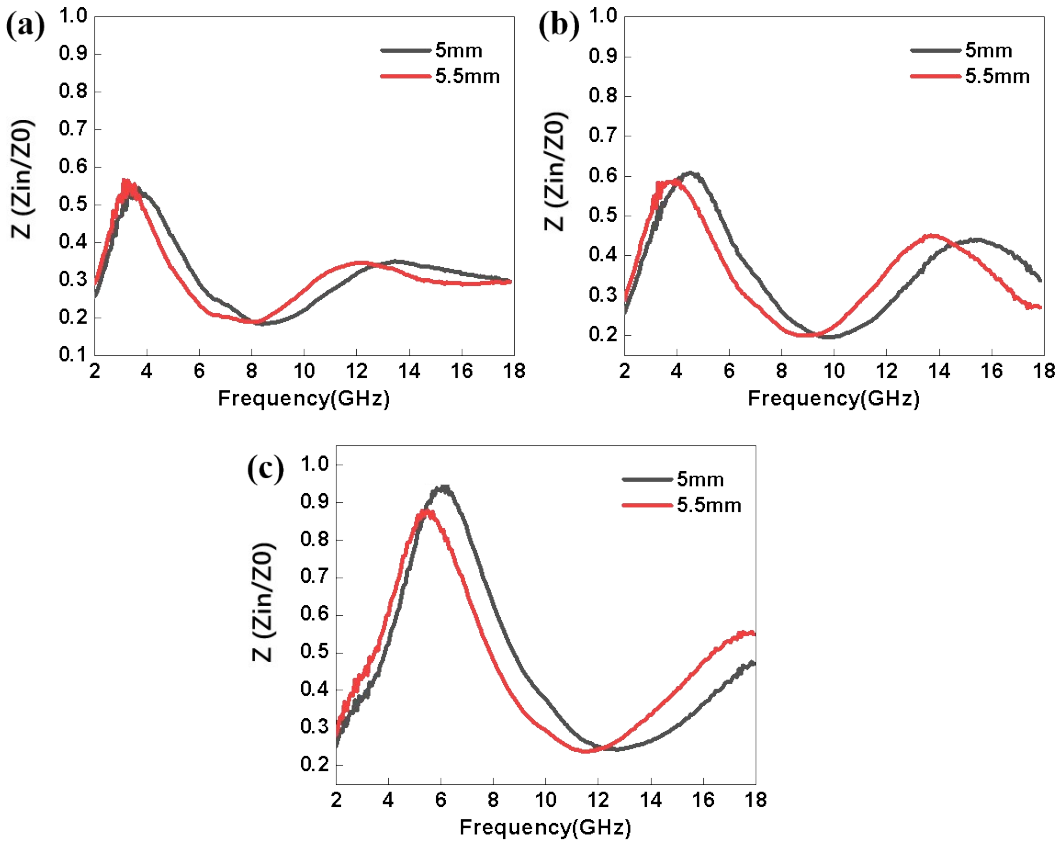

Fig. S11. Z (Z_{in}/Z_0) *versus* frequency at the thickness of 5.0 mm and 5.5 mm: PMPC-1.5 (a), PMPC-2.0 (b) and PMPC-2.5 (c).

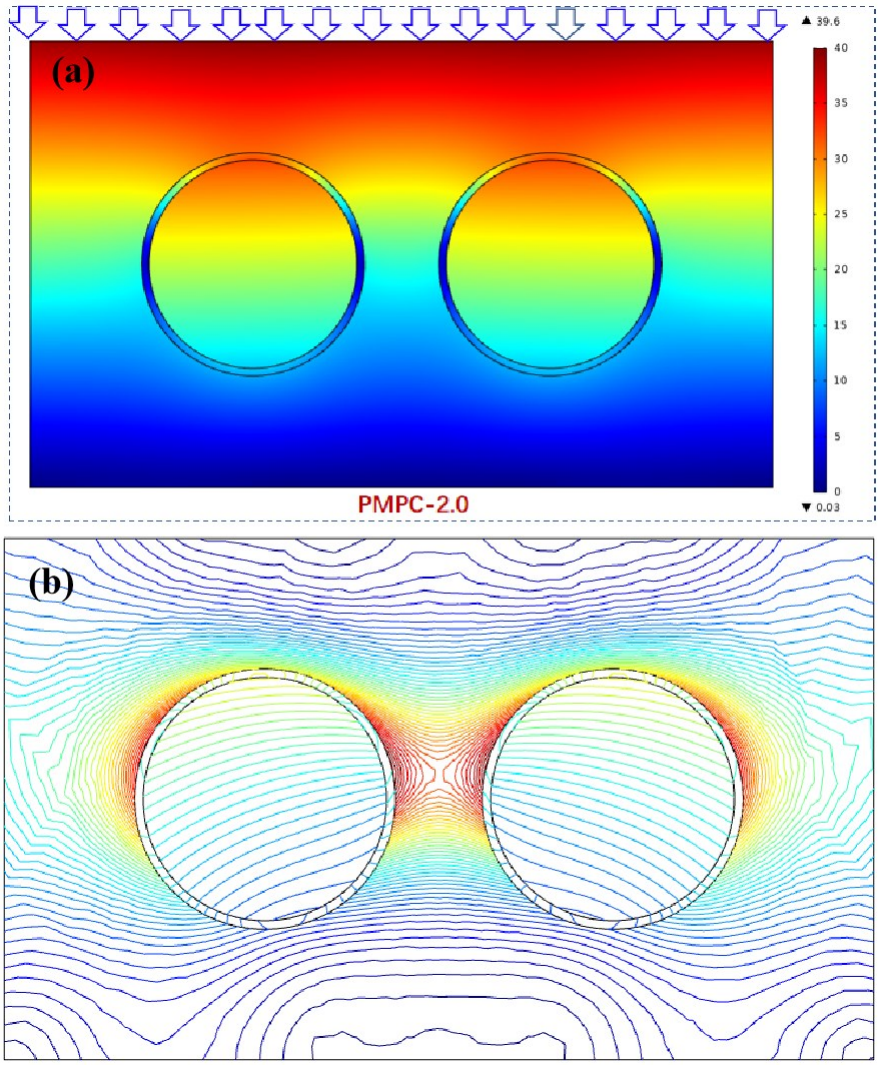

Fig. S12. Numerical simulations of electric field distribution (a) and contour map (b) of PMPC-2.0.

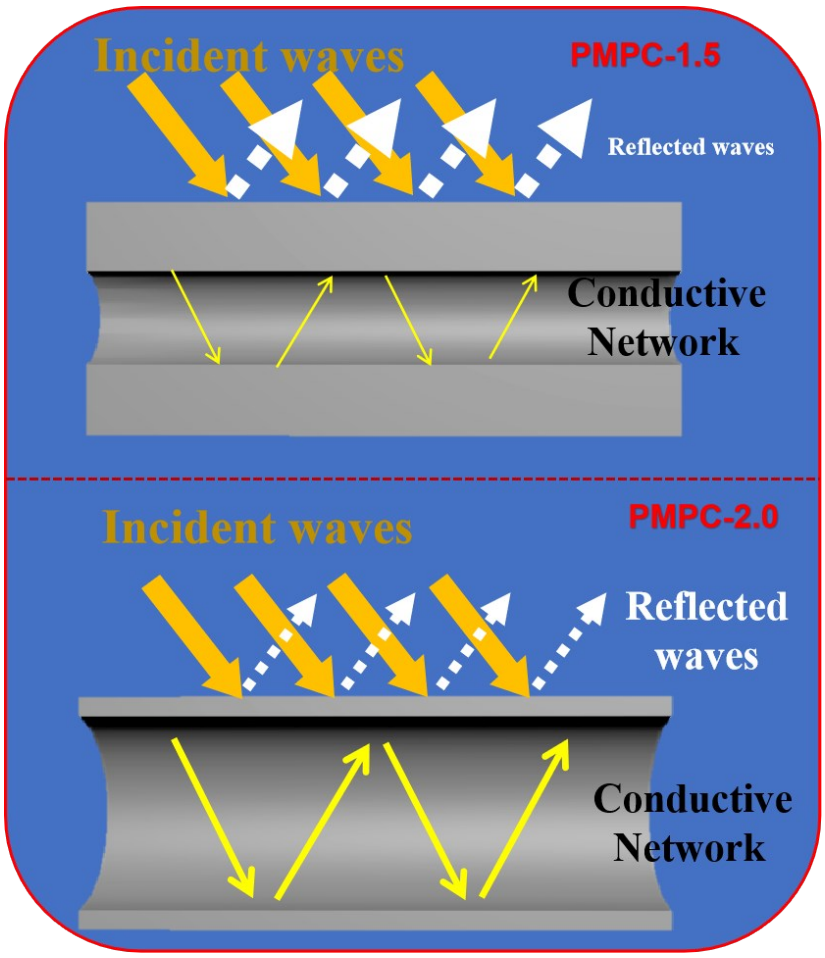

Fig. S13. The absorption mechanisms of PMPC-1.5 and PMPC-2.0.

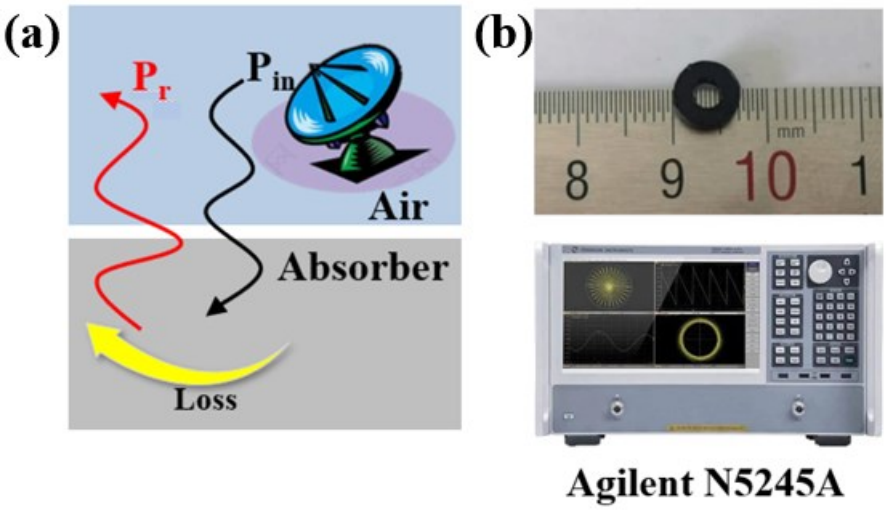

Fig. S14. Schematic illustration of EWA models(a); the photographs of the test sample and instrument (b).

4. Experimental Section

4.1 Preparation of PMPC

The PMPC were synthesized by the In B-E synthesis protocol. Typically, 5.5 mmol glucose were dissolved in 10 ml of deionized (DI) water to form a homogeneous solution. Then, 2.5 g of $Zn(NO_3)_2 \cdot 6H_2O$ was added to this solution under stirring. Then, the homogeneous suspension was heated at 120 ℃ for 2 h. Brown expansion precursor was obtained full of the beaker (100 mL). The resulting precursor was put into a crucible and transferred to the tube furnace. The annealing procedure was set at a temperature of 900℃ for 2 h in N_2 atmosphere with a heating rate of 10℃/min. After cooling down to room temperature, the product was collected from the tube furnace and in no need of any further washing steps.

Different amount of $Zn(NO_3)_2 \cdot 6H_2O$ (1.5 g, 2.0 g) was added to the system to regulate the microcosmic pore configuration of PMPC. And the PMPC were named as PMPC-1.5, PMPC-2.0, PMPC-2.5 according to the amount of $Zn(NO_3)_2 \cdot 6H_2O$.

For comparison, glucose derived carbon was prepared without any $Zn(NO_3)_2 \cdot 6H_2O$ and was shorted as GC.

4.2 Characterization

The crystal structure of the prepared PMPC was characterized by X-ray diffraction (XRD) with a scanning speed of 4°/min from 10° to 90°. A field emission scanning electron microscope of Zeiss was used to observe the micro-morphology of the sample with the operating voltage of 20.00 kV. The specific surface area and pore size analysis of PMPC were analyzed using the ASAP 2000 specific surface. The Renishaw inVia laser micro Raman spectrometer was used to characterize the molecular structure of the material. Thermal stability analysis (nitrogen atmosphere, 30 °C-1000 °C) was performed on the precursor using a NETZSCH thermal analyzer. The conductivity was

measured by a four-probe powder conductivity tester.

4.3 Microwave Absorption Measurements

PMPC and paraffin were mixed under 60 °C. After the mixture was evenly mixed, they were pressed into a circular tube with an outer diameter of 7 mm and an inner diameter of 3 mm to obtain a ring of the same diameter with a thickness of about 2 mm. A vector network analyzer (model Agilent N5245A) was used to test the electromagnetic parameters of the material (Fig. S15). The measurement was performed at room temperature with a measurement range of 2-18 GHz. Subsequently, the relative permittivity ($\varepsilon = \varepsilon' - j\varepsilon''$) and relative permeability ($\mu = \mu' - j\mu''$) in the frequency range of 2-18 GHz can be obtained. Generally, the absorption properties of the absorber are characterized by the reflection loss (RL) value. When an electromagnetic wave is incident from a free space (impedance: Z_0) to an absorbing material (impedance: Z_{in}), the RL values can be calculated based on the transmission line theory.